LncRNA MALAT1 knockdown inhibits cell migration and invasion by suppressing autophagy through miR-384/GOLM1 axis in glioma

R. MA¹, B.-W. ZHANG¹, Z.-B. ZHANG¹, O.-J. DENG²

¹Precision Medicine Center, Tianjin Medical University General Hospital, Tianjin, Heping District, China ²Department of Neurosurgery, Tianjin Medical University General Hospital, Tianjin, Heping District, China

Abstract. – OBJECTIVE: Glioma is characterized by high metastasis with poor outcomes. Long non-coding RNA metastasis associated lung adenocarcinoma transcript 1 (MALAT1) was well-explored in numerous human cancers, including glioma. This study aimed to provide a novel action mechanism of MALAT1 in glioma.

MATERIALS AND METHODS: The expression of MALAT1, microRNA-384 (miR-384) and Golgi membrane protein 1 (GOLM1) was detected by quantitative Real-time polymerase chain reaction (qRT-PCR). The protein levels of GOLM1, light chain3 (LC3-II/LC3-I), p62, Vimentin and E-cadherin were proved by Western blot. Cell migration and invasion were monitored using the transwell assay. Bioinformatics tool star-Base was used to predict target genes and associated binding sites. RNA immunoprecipitation assay (RIP) and dual-luciferase reporter assay were utilized to verify the relationship between miR-384 and MALAT1 or GOLM1. Tumor formation analysis in nude mice was conducted to ascertain the role of MALAT1 in vivo.

RESULTS: MALAT1 was highly expressed in glioma tissues and cells. MALAT1 knockdown inhibited autophagy, migration and invasion of glioma cells. MiR-384 was a target of MALAT1, and miR-384 inhibition reversed the effects of MALAT1 knockdown in glioma cells. GOLM1 was a target of miR-384, and miR-384 inhibition eliminated the function of GOLM1 downregulation in glioma cells. In addition, GOLM1 was regulated by MALAT1 through miR-384. Moreover, MALAT1 knockdown blocked tumor growth and development *in vivo*.

CONCLUSIONS: MALAT1 knockdown depleted migration and invasion by inhibiting autophagy through MALAT1/miR-384/GOLM1 axis in glioma in vitro and *in vivo*. The MALAT1/miR-384/GOLM1 axis was first proposed in our report, enriching the action mechanism of MALAT1 in glioma.

Key Words.

MALAT1, MiR-384, GOLM1, Glioma, Autophagy, Migration, Invasion.

Introduction

Glioma is the most common primary malignancy in the central nervous system ¹. The morbidity and mortality of glioma have remained high due to the highly complex molecular genetic traits ^{2,3}. Glioma can be classified into four grades, and high-grade glioma is challenging to treat because of invasiveness and lethality, leading to recurrence after surgery^{4,5}. Although advances in a variety of treatments have made, including surgical resection, radiation therapy, and chemotherapy, the survival rate of glioma patients within 5 years is still unsatisfactory^{6,7}. Therefore, further exploration of the molecular mechanisms of glioma development and progression and more appropriate therapeutic targets will provide additional options for glioma treatment.

The role of autophagy in cancer varies from case to case. On the one hand, autophagy plays a vital role in the maintenance of cellular homeostasis. Therefore, autophagy mediates the role of tumor suppression^{8,9}. On the other hand, autophagy also maintains the survival and proliferation of tumor cells in specific environments, thus supporting tumor growth, invasion and metastasis¹⁰⁻¹². The activation of autophagy is identified according to the expression of specific autophagy marker proteins, including beclin-1, light chain 3 (LC3) and p62¹³. As markers of the autophagosome, the protein levels of LC3-II and p62 represent the amount of autophagosome. Invasion of glioma cells into surrounding tissues is one of the leading causes of poor survival due to treatment failure¹⁴. Glioma cells have a significant ability to infiltrate the brain and can migrate long distances from the primary tumor, which poses a considerable challenge for complete surgical resection¹⁵. Especially, autophagy was reported to be closely associated with cell migration and invasion in human cancers¹⁶. Hence, the determination of autophagy will be helpful in understanding cancer cell migration and invasion.

Long non-coding RNA (lncRNA) is one of the non-coding RNAs with over 200 nucleotides. It is universally acknowledged that lncRNAs are implicated in the development of cancers. In glioma, several lncRNAs, such as OIP5-AS1, DAN-CR and DLX6-AS1, were proved to play crucial roles in cell cycle, apoptosis, drug resistance, invasion, migration and tumor growth¹⁷⁻¹⁹. Metastasis associated lung adenocarcinoma transcript 1 (MALAT1) was widely mentioned in dozens of cancers, including cervical cancer, tongue squamous cell carcinoma, and ovarian cancer²⁰⁻²². Acting as an oncogene, its role was gradually determined. However, the function of MALAT1 on autophagy in glioma is still limited.

LncRNAs regulate stability and translation of message RNAs (mRNAs) by serving as a precursor to microRNAs (miRNAs) or acting as competitive endogenous RNAs (CeRNAs)²³. MiRNAs are short non-coding RNAs (ncRNAs) with ~22 nucleotides²⁴. Recently, the role of miR-384 was investigated in details, serving as a tumor suppressor to block tumor progression^{25,26}. Interestingly, the research of miR-384 in glioma has proceeded and made us realize the role of miR-384 in glioma^{27,28}. Indeed, the characterization of miR-384 in glioma is still inadequate, and the associated mechanism is lacking. Generally, miRNAs modulate gene expression at post-transcriptional and translational levels via binding to the specific binding site in 3' untranslated region (3' UTR) of targeted mRNAs²⁹. Golgi membrane protein 1 (GOLM1) also plays a vital role in tumorigenesis and progression of cancers, including prostate cancer, lung cancer and glioma³⁰⁻³². Unfortunately, the effect of GOLM1 on autophagy is hard to find, and its action mechanism in glioma needs further exploring.

In our present study, the expression level of MALAT1 in glioma tissues and cell lines was detected, and the role of MALAT1 on autophagy, migration and invasion was investigated *in vitro* and *in vivo*. The purpose of this study was to observe the role of MALAT1 in glioma and provide a novel mechanism of glioma metastasis.

Materials and Methods

Tissues and Cell Lines

A total of 25 glioma patients and 25 healthy volunteers were recruited from Tianjin Medi-

cal University General Hospital. Tumor tissues (n=25) from glioma patients and normal tissues (n=25) from healthy volunteers were placed in liquid nitrogen and stored at -80°C condition. Informed consent was obtained from each subject before surgery. This research was authorized by the Ethics Committee of Tianjin Medical University General Hospital.

Glioma cells (SHG-44) were purchased from BeNa Culture Collection (Suzhou, China). Another Glioma cells (LN229), cerebral microvascular endothelium (HBEC-5i) and 293T cells were obtained from American Type Culture Collection (ATCC, Manassas, VA, USA). All cells were maintained in Dulbecco's modified Eagle's medium (DMEM) (Life Technologies, Waltham, MA, USA) supplemented with 10% fetal bovine serum (FBS; Life Technologies) in a humidified condition with 5% CO, at 37 °C.

Quantitative Real-Time Polymerase Chain Reaction (qRT-PCR)

Total RNA from tissues and cells was extracted using TRIzol reagent (TaKaRa, Dalian, China) and detected by NanoDrop 2000 spectrophotometers (Thermo Fisher Scientific, Waltham, MA, USA). Then complementary DNA (cDNA) was assembled using TIANScript RT Kit (Tiangen, Beijing, China) and miRcute miRNA First-Strand cDNA Synthesis Kit (Tiangen). Next, FastFire qPCR PreMix (SYBR Green) (Tiangen) was used to perform gRT-PCR under ABI 7500 Thermocycler (Thermo Fisher Scientific). Relative expression was calculated using the 2-ΔΔCt method and calibrated by β-actin or small nuclear RNA U6. The primers were listed as follows: MALAT1, F: 5'-TGATAGCCAAATTGAGACAA-3' and R: 5'-TTCAGGGTGAGGAAGTAAAA-3'; miR-384, F: 5'-TGTTAAATCAGGAATTTTAA-3' and R: 5'-TGTTACAGGCATTATGAA-3'; GOLM1, F: 5'-CCGGAGCCTCGAAAAGAGATT-3' and R: 5'-ATGATCCGTGTCTGGAGGTC-3'; β-actin, F: 5'- ATGGGTCAGAAGGATTCCTATGTG-3' and R: 5'- CTTCATGAGGTAGTCAGTCAG-GTC-3'; U6, F: 5'-CTCGCTTCGGCAGCAG-CACATATA-3' and R: 5'-AAATATGGAAC-GCTTCACGA-3'.

Western Blot

Total proteins were isolated from tissues and cells using Radio Immunoprecipitation Assay (RIPA) buffer (Beyotime, Shanghai, China) and then electrophoresed by 12% sodium dodecyl sulfate-polyacrylamide gel electrophoresis (SDS-PAGE) and

electro-transferred onto polyvinylidene difluoride (PVDF) membranes (Bio-Rad, Hercules, CA, USA) on ice. Subsequently, the membranes were placed in a blocking solution (phosphate-buffered saline (PBS) containing 5% skim milk) for 2 h and next probed with the primary antibodies against LC3B (1:500, 18725-1-AP; Proteintech Group; Chicago, IL, USA), p62 (1:1000, 18420-1-AP; Proteintech Group), Vimentin (1:5000, 10366-1-AP; Proteintech Group), E-cadherin (1:5000, 20874-1-AP; Proteintech Group), GOLM1 (1:1000, 15126-1-AP; Proteintech Group) and β-actin (1:2000, 20536-1-AP; Proteintech Group) at 4°C overnight. The next day, the membranes were probed by the horseradish peroxidase (HRP)-labeled secondary antibody (1:2000, 15134-1-AP; Proteintech Group) at room temperature for 2 h. Finally, protein blot signals were visualized using the enhanced chemiluminescence (ECL) detection kit (Beyotime, Shanghai, China).

Cell Transfection

Small interference RNA (si-RNA) against MALAT1 (si-MALAT1), siRNA against GOLM1 (si-GOLM1) and siRNA negative control (si-NC) were assembled by Sangon Biotech (Shanghai, China). MiR-384 mimic, miR-384 inhibitor and their separate control (miR-NC or anti-miR-NC) were obtained from Ribobio (Guangzhou, China). Cell transfection was executed using Lipofectamine 2000 (Invitrogen, Carlsbad, CA, USA) based on the product's instruction.

Transwell Assay

The transfected LN229 and SHG-44 cells were harvested, resuspended in serum-free DMEM containing 10% FBS and placed into the upper 24-well transwell chambers (Corning Inc.; Corning, NY, USA) for migration assay or chambers coated with Matrigel (Corning) for invasion assay. Meanwhile, DMEM mixed with 10% FBS was added into the lower chambers. After 24 h, the migrated or invaded cells on the lower surface were fixed with 4% paraformaldehyde (PFA) and stained with methanol containing 0.1% crystal violet for 15 min. Then, five randomly selected fields were taken to calculate cell amounts using an Olympus microscope (Olympus, Tokyo, Japan) at a magnification of × 100.

Bioinformatics Prediction and Dual-Luciferase Reporter Assay

The targets of lncRNA or miRNA were predicted by the online bioinformatics tool starBase (http://starbase.sysu.edu.cn).

To verify the relationship between miR-384 and MALAT1 or GOLM1, dual-luciferase reporter assay was carried out. In brief, MALAT1 wild-type (MALAT1 WT) sequences containing the binding site with miR-384 and corresponding MALAT1 mutant (MALAT1 MUT) sequences were respectively constructed onto the downstream of pmirGLO vectors (Promega, Madison, WI, USA) to assemble fusion plasmid, named as MALAT1 WT and MALAT1 MUT. Afterward, MALAT1 WT or MALAT1 MUT and miR-384 mimic were co-inserted into 293T cells. Dual-luciferase assay system (Promega) was used to detect luciferase activities in 293T cells at 48 h after transfection. The wild-type 3' UTR sequences of GOLM1 containing the binding site with miR-384 and corresponding GOLM1 3' UTR mutant (GOLM1 MUT) sequences were also amplified and cloned into pmirGLO (Promega) to generate GOLM1 WT or GOLM1 MUT luciferase reporter vector, respectively. Then, the following experiments were executed as mentioned above.

RNA Immunoprecipitation Assay (RIP)

Magna RNA-binding protein immunoprecipitation kit (Millipore, Billerica, MA, USA) was utilized to execute RIP assay in line with the manufacturer's protocol. Briefly, LN229 and SHG-44 cells were collected and exposed to RNA lysis buffer. Then, cell lysate was cultured with RIP buffer containing human Ago2 antibody and mouse IgG (control). Later, immunoprecipitated RNA was extracted, and qRT-PCR was conducted as the above-mentioned to detect the level of MALAT1 and miR-384.

In Vivo Experiments

Mice experiments were approved by the Animal Care and Use Committee of Tianjin Medical University General Hospital. A total of 12 nude mice were purchased from HFK bioscience (Beijing, China) and divided into 2 groups (n=6). Lentiviral vector (lenti-short hairpin sh-MALAT1) and its negative control (sh-NC) were obtained from Genechem (Shanghai, China) and introduced into LN229 cells for stable MALAT1 knockdown. After 48 h, transfected LN229 cells were injected into the right flank of mice groin. Subsequently, the mice were kept for 7 days, and next, the tumor volume was recorded every 5 days according to the formula: volume=length × width $^2 \times 0.5$. 35 days later, all mice were killed, and the tumors were removed for weighting and other molecular investigations.

Statistical Analysis

GraphPad Prism v5.01 (GraphPad Software, La Jolla, CA, USA) was used for data processing. All data from 3 independent biological replications were presented as the mean \pm standard deviation (SD). Difference analysis was performed using the Student's *t*-test between 2 groups and oneway analysis of variance among multiple groups, and Bonferroni post-hoc analysis was conducted. The Spearman rank correlation coefficient was utilized to determine the correlation between the two parameters. Differences were regarded as statistically significant when p < 0.05.

Results

MALAT1 Was Enriched in Glioma Tissues and Cells, and Autophagy Was Activated in Glioma Tissues and Cells

The expression of MALAT1 and autophagy-related proteins were monitored in glioma tissues and cells by qRT-PCR or Western blot. The result showed that the expression of MALAT1 was significantly enhanced in tumor tissues (n=25) relative to normal tissues (n=25) (Figure 1A). Besides, the increased protein level of LC3-II and the decreased protein level of p62 were observed

in glioma tissues rather than that in normal tissues (Figure 1B). Likewise, the expression of MALAT1 in LN229 and SHG-44 cells was notably higher than that in HBEC-5i cells (Figure 1C). The protein level of LC3-II in LN229 and SHG-44 cells was elevated, while the level of p62 in LN229 and SHG-44 cells was reduced relative to HBEC-5i cells (Figure 1D). The data suggested that MALAT1 was up-regulated in glioma, and autophagy was activated in glioma.

MALAT1 Knockdown Inhibited Cell Migration and Invasion via Restricting Autophagy

The endogenous level of MALAT1 was reduced in LN229 and SHG-44 cells by transfecting with si-MALAT1 to ascertain the role of MALAT1 in glioma *in vitro*. First, the qRT-PCR analysis exhibited that the expression of MALAT1 was obviously decreased in LN229 and SHG-44 cells transfected with si-MALAT1 (Figure 2A). Besides, the Western blot analysis exposed that the level of LC3-II was rapidly decreased in LN229 and SHG-44 cells with the knockdown of MALAT1, while the level of p62 was reinforced (Figure 2B). Moreover, the number of migrated or invaded cells was investigated, and the result indicated that cell migration and in-

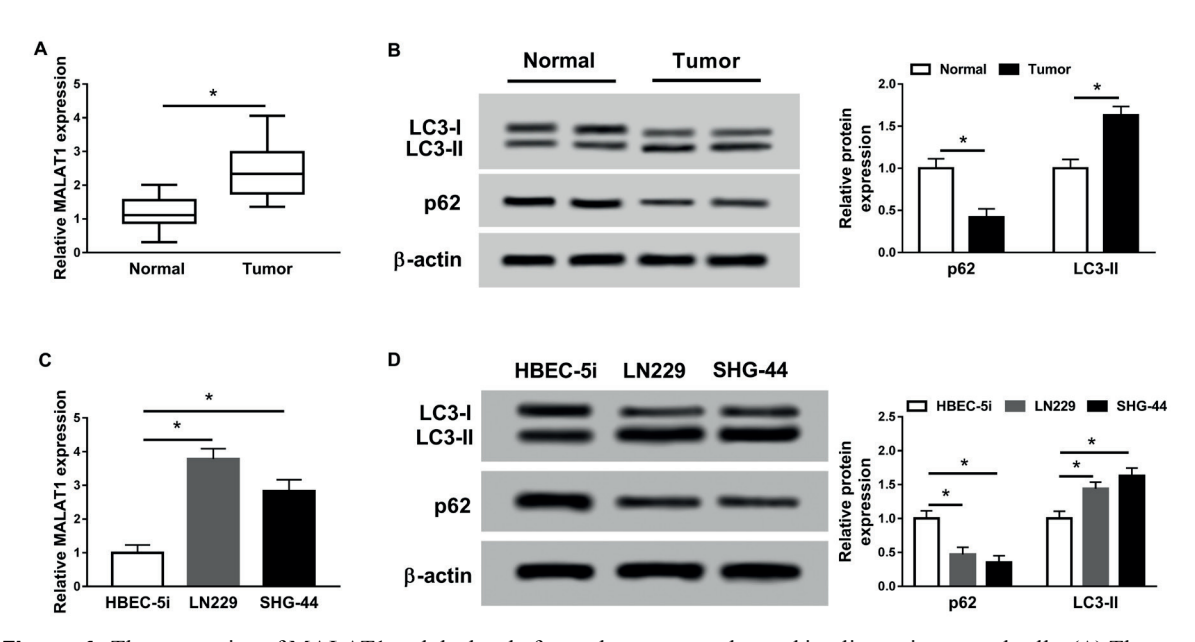


Figure 1. The expression of MALAT1 and the level of autophagy were enhanced in glioma tissues and cells. **(A)** The expression of MALAT1 in tumor tissues and normal tissues was detected by qRT-PCR. **(B)** The protein levels of LC3-II and p62 in tumor tissues and normal tissues were quantified by Western blot. **(C)** The expression of MALAT1 in LN229, SHG-44 and HBEC-5i cells was measured by qRT-PCR. **(D)** The protein levels of LC3-II and p62 in LN229, SHG-44 and HBEC-5i cells were quantified by Western blot. *p < 0.05.

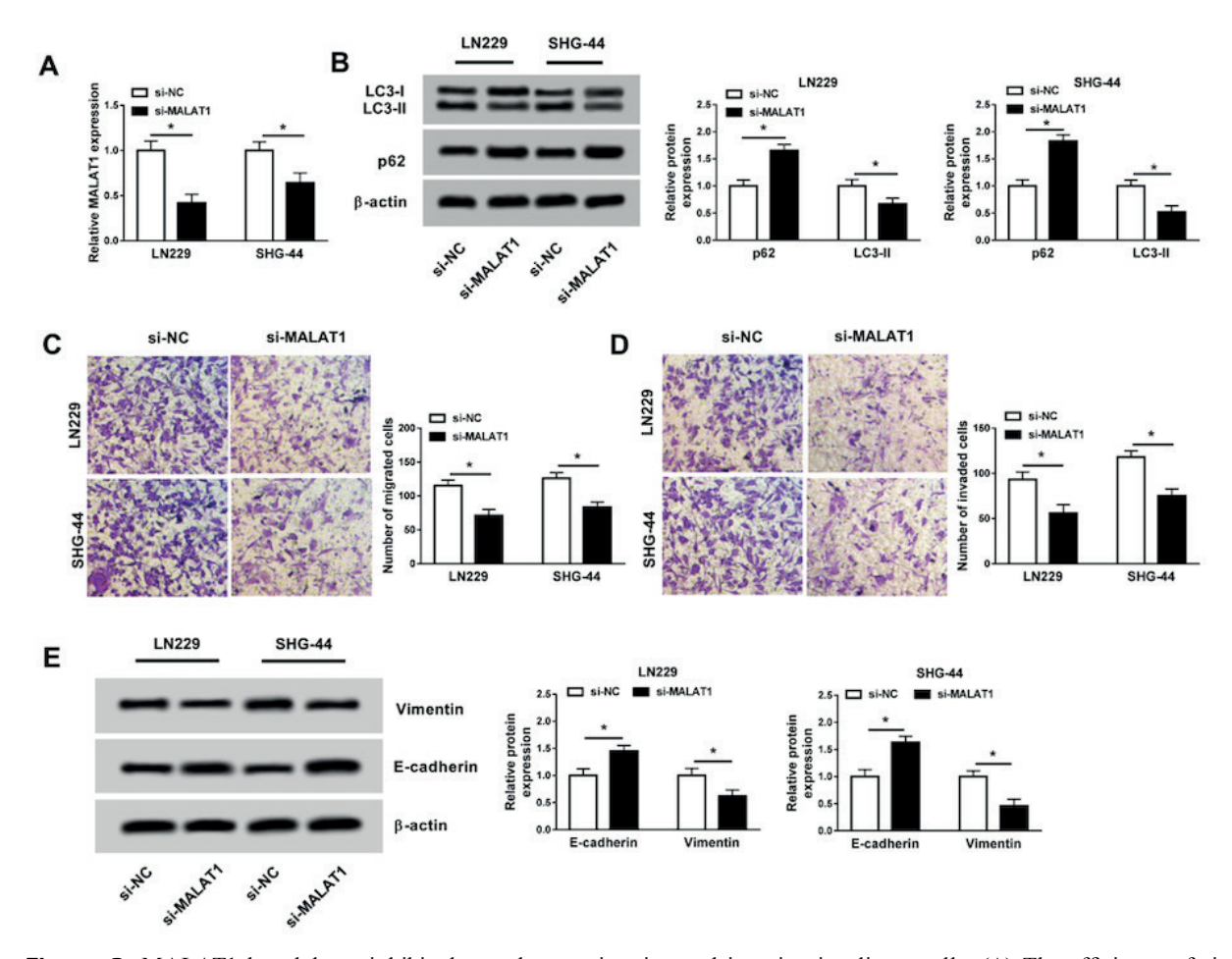


Figure 2. MALAT1 knockdown inhibited autophagy, migration and invasion in glioma cells. **(A)** The efficiency of si-MALAT1 transfection in LN229 and SHG-44 cells was monitored by qRT-PCR. **(B)** The protein levels of LC3-II and p62 in LN229 and SHG-44 cells transfected with si-MALAT1 or si-NC were assessed by Western blot. **(C** and **D)** The migration and invasion of LN229 and SHG-44 cells transfected with si-MALAT1 or si-NC were detected using transwell assay (100×). **(E)** The protein levels of Vimentin and E-cadherin were measured using Western blot. *p < 0.05.

vasion were blocked in LN229 and SHG-44 cells transfected with si-MALAT1 (Figure 2C and 2D). Additionally, the expression of epithelial-mesenchymal transition (EMT) markers (Vimentin and E-cadherin) was determined, and we discovered that the level of E-cadherin was prominently enhanced, while the level of Vimentin was sharply declined with the knockdown of MALAT1 in LN229 and SHG-44 cells (Figure 2E). These data revealed that MALAT1 knockdown weakened the ability of migration and invasion through mediating autophagy in glioma cells.

MALAT1 Acted as a Sponge of miR-384

The candidate miRNAs with complementary sequences to MALAT1 were predicted using online the bioinformatics tool starBase. MiR-384 was one of these predicted targets and was

down-regulated in glioma tissues or cells (LN229 and SHG-44) relative to normal tissues or cells (HBE-5i) (Figure 3A and 3B). Besides, the expression levels of miR-384 in glioma tissues were negatively correlated with the expression of MALAT1 (Figure 3C). To further verify the relationship between MALAT1 and miR-384, RIP assay was performed and showed higher levels of MALAT1 and miR-384 in the Anti-Ago2 group compared with that in the Anti-IgG group (Figure 3D). In addition, the binding site of MALAT1 and miR-384 was obtained by starBase and used for dual-luciferase reporter assay. The result showed that miR-384 mimic pronouncedly reduced the luciferase activity in 293T cells transfected with MALAT1 WT but did not alter the luciferase activity in 293T cells transfected with MALAT1 MUT (Figure 3E). Furthermore, the expression

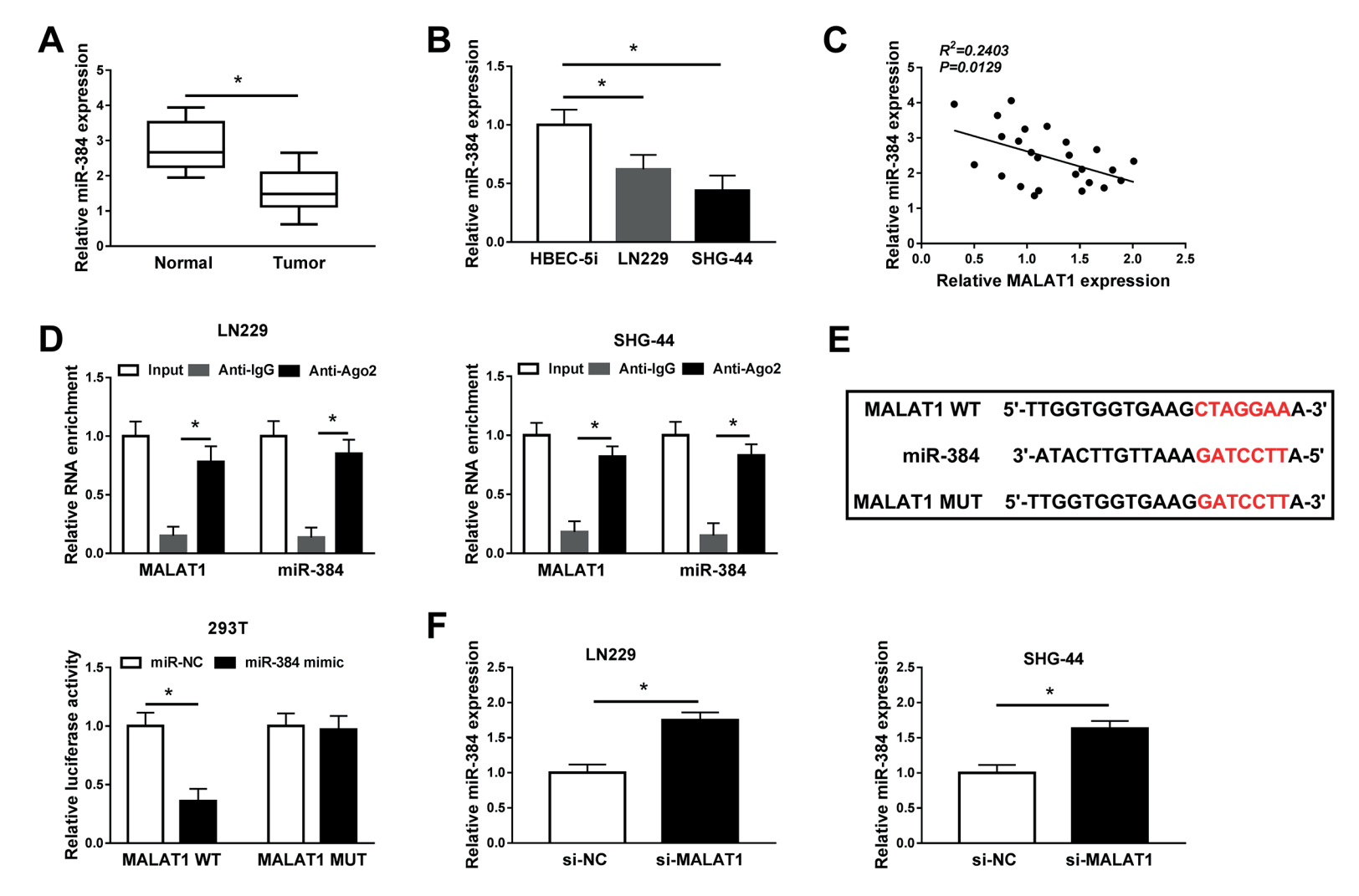


Figure 3. MiR-384 was a target of MALAT1. (**A** and **B**) The expression of miR-384 in glioma tissues and cell lines was monitored by qRT-PCR. (**C**) The correlation between miR-384 expression and MALAT1 expression in glioma tissues was assessed following the Spearman rank correlation coefficient. (**D** and **E**) The relationship between miR-384 and MALAT1 was verified by RIP assay and dual-luciferase reporter assay. (**F**) The expression of miR-384 was examined in LN229 and SHG-44 cells transfected with si-MALAT1 or si-NC. *p < 0.05.

of miR-384 was enhanced with the weak level of MALAT1 in LN229 and SHG-44 cells (Figure 3F). The above data showed that MALAT1 could directly bind to miR-384.

Inhibition of miR-384 Reversed the Regulatory Effects Mediated by MALAT1 Knockdown

Rescue experiments were conducted to observe whether MALAT1 functioned by sponging miR-384. LN229 and SHG-44 cells were introduced with si-MALAT1, si-NC, si-MALAT1+miR-384 inhibitor or si-MALAT1+anti-miR-NC. transfection efficiency was monitored through observing the expression of miR-384, and the result exhibited that the expression miR-384 was significantly strengthened in the si-MALAT1 group but repressed in the si-MALAT1+miR-384 inhibitor group (Figure 4A). Western blot analysis showed that the level of LC3-II, inhibited by MALAT1 knockdown, was recovered by miR-384 inhibition. On the contrary, the levels of p62, stimulated by MALAT1 knockdown, were suppressed by miR-384 inhibition (Figure 4B). In addition, the number of migrated and invaded cells, blocked in the si-MALAT1 transfection group, was restored in the si-MALAT1+miR-384 inhibitor transfection group (Figure 4C and 4D). Not surprisingly, the expression level of Vimentin was restrained in the si-MALAT1 group but elevated in the si-MALAT1+miR-384 inhibitor group, while the expression of E-cadherin was promoted by MALAT1 knockdown but inhibited by miR-384 inhibition (Figure 4E). These data hinted that MALAT1 regulated autophagy, migration and invasion through sponging miR-384.

GOLM1 Was a Downstream Target of miR-384

The putative target genes of miR-384 were predicted by starBase. GOLM1 was one of several targets of miR-384 and was markedly up-regulated in glioma tissues relative to normal tissues at mRNA and protein levels (Figure 5A and 5B). Moreover, the expression of GOLM1 in LN229 and SHG-44 cells was also reinforced relative to HBEC-5i cells at both mRNA and protein levels (Figure 5C and 5D). The mRNA level of GOLM1 was negatively correlated with miR-384 expression level in glioma tissues (Figure 5E). Subsequently, the GOLM1 3' UTR wild-type sequences containing the binding site with miR-384 and mutated GOLM1 3' UTR mutant sequences were obtained by the analysis of starBase for dual-lu-

ciferase reporter assay, and the consequence presented that the luciferase activity in 293T cells cotransfected with miR-384 mimic and GOLM1 3' UTR-WT was strikingly reduced compared with miR-NC, while the luciferase activity in 293T cells cotransfected with miR-384 mimic and GOLM1 3' UTR-MUT had no noticeable difference compared with miR-NC (Figure 5F). Moreover, the expression of GOLM1 at the protein level was declined with the enrichment of miR-384 in LN229 and SHG-44 cells (Figure 5G). The above-mentioned data indicated that GOLM1 was a target of miR-384.

The Regulatory Effects of GOLM1 Knockdown Were Eliminated by miR-384 Inhibition

To investigate whether miR-384 inhibited the role of GOLM1 in glioma cells, si-GOLM1, si-NC, si-GOLM1+miR-384 inhibitor and si-GOLM1+anti-miR-NC were introduced into LN229 and SHG-44 cells, respectively. The expression of GOLM1 at the protein level was monitored to assess transfection efficiency (Figure 6A). The expression of GOLM1 was decreased in LN229 and SHG-44 cells transfected with si-GOLM1 but recovered with the transfection of si-GOLM1+miR-384 inhibitor. The level of LC3-II was decreased with the knockdown of GOLM1 but regained with the inhibition of miR-384, while the level of p62 was opposite to the expression of LC3-II (Figure 6B). Transwell assay elucidated that the number of migrated or invaded cells was depleted in the si-GOLM1 group but enhanced in the si-GOLM1+miR-384 inhibitor group compared with their corresponding controls (Figure 6C and 6D). Additionally, the level of Vimentin was declined in LN229 and SHG-44 cells transfected with si-GOLM1, while the level of E-cadherin was elevated. However, the level of Vimentin was strengthened in LN229 and SHG-44 cells transfected with si-GOLM1+miR-384 inhibitor, while the level of E-cadherin was reduced (Figure 6E). These results indicated that miR-384 inhibition could reverse the GOLM1 knockdown-mediated effect on cell activities.

MALAT1 Regulated the Expression of GOLM1 Through miR-384

The expression of GOLM1 at mRNA and protein levels was examined in si-MALAT1, si-NC, si-MALAT1+miR-384 inhibitor or si-MALAT1+anti-miR-NC transfected LN229 and SHG-44 cells. The result manifested that the ex-

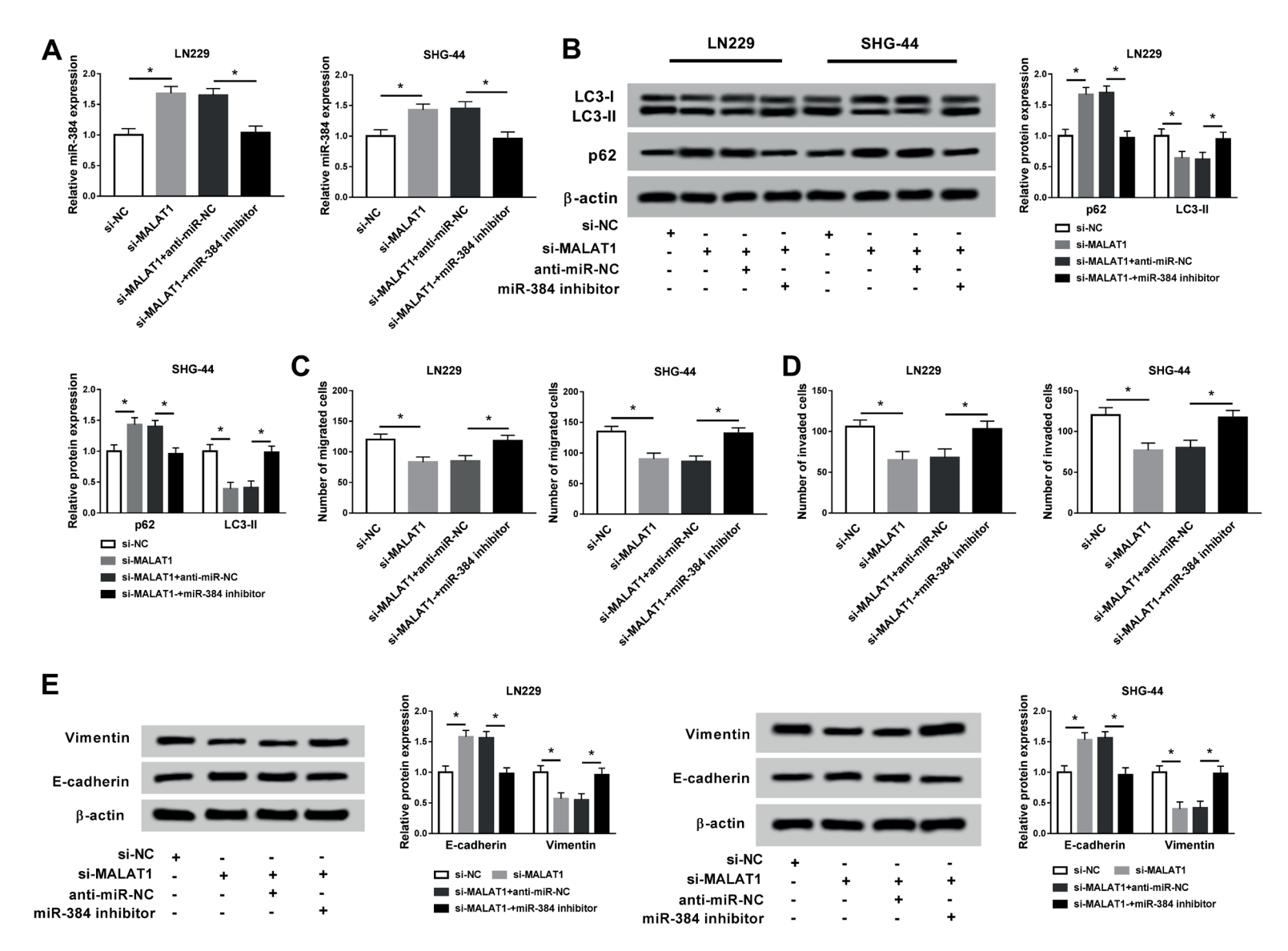


Figure 4. MiR-384 inhibition reversed the effects of MALAT1 knockdown on autophagy, migration and invasion in glioma cells. LN229 and SHG-44 cells were transfected with si-MALAT1 or si-MALAT1+miR-384 inhibitor, si-NC or si-MALAT1+anti-miR-NC as the control. **(A)** The transfection efficiency was detected by qRT-PCR. **(B)** The protein levels of p62 and LC3-II were monitored by Western blot. **(C** and **D)** The migration and invasion were assessed by transwell assay ($100 \times$). **(E)** The expression of Vimentin and E-cadherin at the protein level was quantified by Western blot. *p < 0.05.

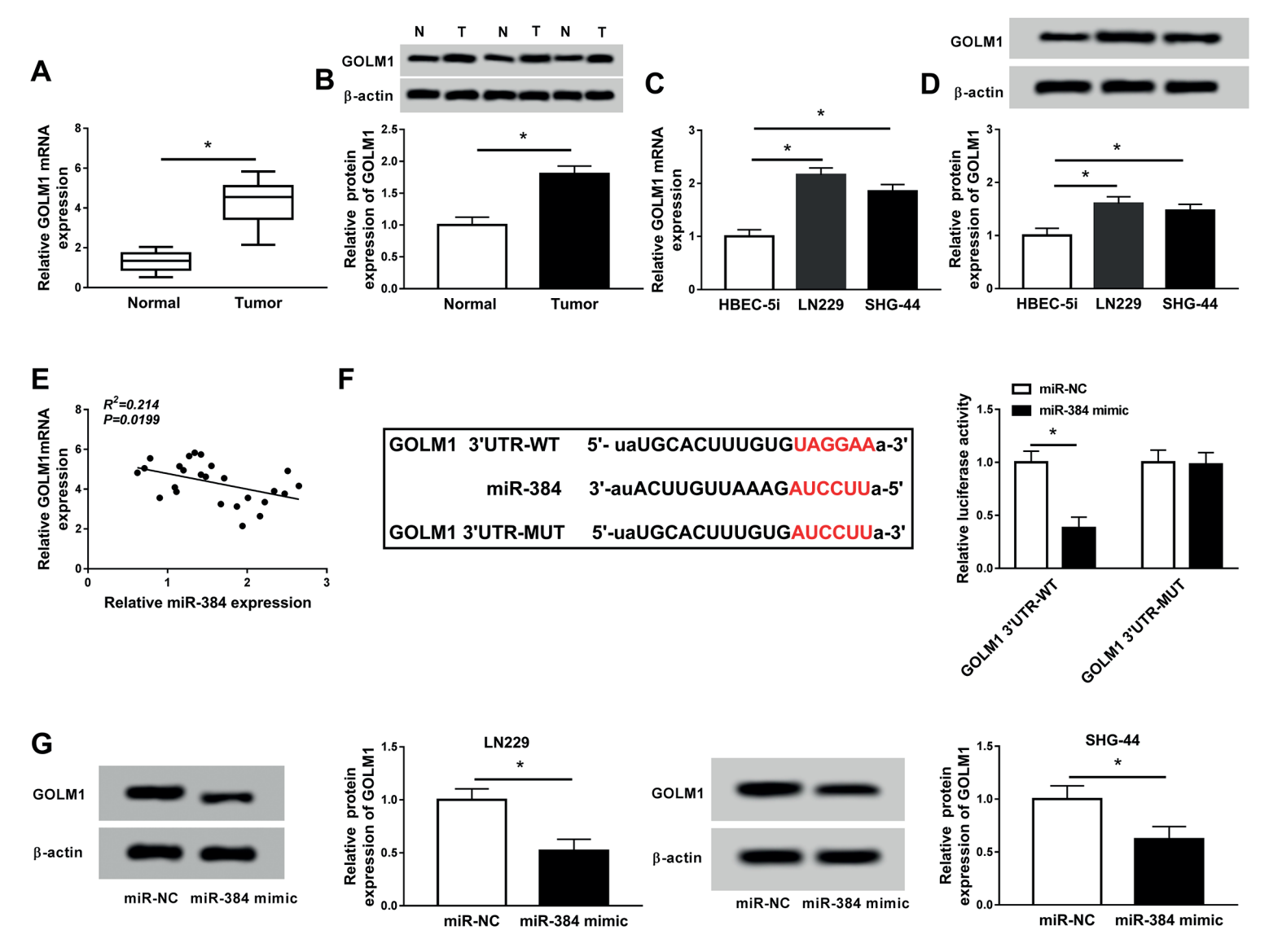


Figure 5. GOLM1 was a target of miR-384. **(A-D)** The expression of GOLM1 at mRNA and protein levels in glioma tissues and cells was detected by qRT-PCR and Western blot. **(E)** The correlation between GOLM1 expression and miR-384 expression in glioma tissues was established according to the Spearman rank correlation coefficient. **(F)** The relationship between GOLM1 and miR-384 was confirmed using the dual-luciferase reporter assay. **(G)** The expression of GOLM1 at the protein level was quantified by Western blot. *p < 0.05.

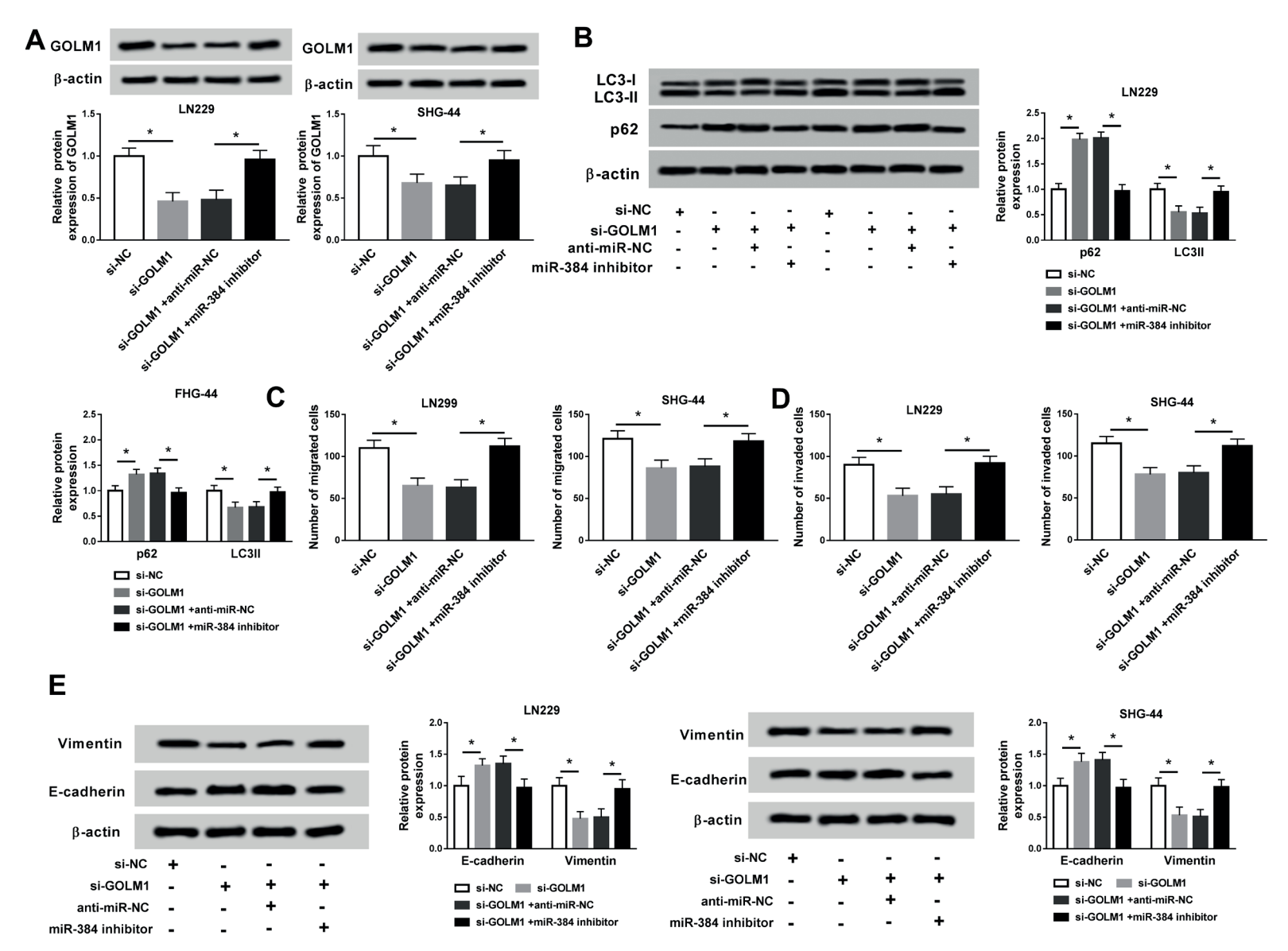


Figure 6. MiR-384 inhibition abolished the role of GOLM1 downregulation on autophagy, migration and invasion in glioma cells. LN229 and SHG-44 cells were introduced with si-GOLM or si-GOLM+miR-384 inhibitor, si-NC or si-GOLM+anti-miR-NC as the control. **(A)** The transfection efficiency was examined using qRT-PCR. **(B)** The protein levels of p62 and LC3-II were monitored by Western blot. **(C** and **D)** The migration and invasion were assessed by transwell assay ($100\times$). **(E)** The expression of Vimentin and E-cadherin at the protein level was quantified by Western blot. *p < 0.05.

pression of GOLM1 was substantially diminished with the transfection of si-MALAT1 compared with si-NC but steeply recovered with the transfection of si-MALAT1+miR-384 inhibitor compared with si-MALAT1+anti-miR-NC (Figure 7A and 7B), indicating that the expression of GOLM1 was modulated by MALAT1 through miR-384.

MALAT1 Downregulation Inhibited Tumor Growth in Vivo

Xenograft models were established to assess the role of MALAT1 in vivo. The tumor volume and weight in the experimental group (sh-MALAT1) were notably weaker than those in the control group (sh-NC) (Figure 8A and 8B). The analysis of Western blot showed that the level of LC3-II was significantly decreased, while the level of p62 was inversely elevated in tumor tissues from the sh-MALAT1 group relative to the sh-NC group (Figure 8C). Besides, the expression of MALAT1 was lower in the sh-MALAT1 group than that in the sh-NC group, while the expression of miR-384 exhibited higher expression in the sh-MALAT1 group. The expression of GOLM1 at mRNA and protein levels was suppressed in the sh-MALAT1 group relative to the sh-NC group (Figure 8D and 8E). Furthermore, the level of Vimentin was noticeably weakened in the sh-MALAT1 group, while the level of E-cadherin was visibly enhanced in the sh-MALAT1 group relative to sh-NC group (Figure 8F). These data proved that MALAT1 downregulation inhibited tumor growth and autophagy in vivo, leading to the block of migration and invasion.

Discussion

Glioma is characterized by high metastasis, resulting in treatment obstacles and poor prognosis. Advanced human tumors are often accompanied by increased autophagy flux, which is associated with metastatic and invasive phenotypes and poor prognosis ³³. Therefore, it is of considerable significance for the treatment of glioma to explore the metastasis and invasion of glioma through autophagy. In this paper, we reported that MALAT1 was aberrantly up-regulated in glioma tissues and cells, and MALAT1 downregulation sequestered cell migration and invasion by blocking autophagy. Mechanism analysis concluded that miR-384 was a target of MALAT1 and interacted with the 3' UTR of GOLM1. Inhibition of miR-384 reversed or abolished the effects of MALAT1

knockdown or GOLM1 knockdown in glioma cells. The targeting relationship between miR-384 and MALAT1 or GOLM1 was identified in this work for the first time.

MALAT1 is highly conserved and enriched in the nucleus³⁴. An increasing number of studies have expounded the role of MALAT1 in glioma. In particular, Li et al³⁵ demonstrated that the expression of MALAT1 was enriched in glioma cells, and MALAT1 knockdown could suppress proliferation and accelerate apoptosis. Han et al³⁶ maintained that MALAT1 downregulation regulated the activity of stemness markers and cell proliferation in glioma stem cells. Xiang et al³⁷ put forward that MALAT1 was highly expressed in glioma tissues and cells, and cell viability was declined with MALAT1 knockdown, while the apoptosis rate was drastically promoted. Consistent with these studies, the expression of MALAT1 was also reinforced in glioma tissues and cells through our analysis. However, the function of MALAT1 on autophagy in glioma was weakly explored. Only a previous report manifested that MALAT1 activated autophagy, leading to an increase of cell proliferation. Besides, 3-MA-inhibited autophagy weakened MALAT1-mediated proliferation³⁸. Similarly, in our research, MALAT1 knockdown relieved autophagy activity, leading to the inhibition of cell migration and invasion, suggesting the carcinogenic effect of MALAT1 in glioma.

To determine the action mechanism of MALAT1, the putative target miRNAs of MALAT1 were forecasted and verified. MiR-384 was screened and identified as one of its targets, and its function in glioma was partly detected. Gu et al²⁷ summarized that miR-384 was poorly expressed in glioma tissues, and the reintroduction of miR-384 significantly sustained glioma cell proliferation, migration and invasion. Zheng et al²⁸ elucidated that miR-384 exerted tumor-suppressive role in glioma cells and invalidated lncRNA CRNDE-mediated tumor malignant progression. In agreement with their data, we discovered that miR-384 expressed with a low level in glioma tissues and cell lines. Inhibition of miR-384 reversed the regulatory effects of MALAT1 knockdown on autophagy, migration and invasion.

To further explore the action mechanism of MALAT1, the downstream target mRNAs of miRNAs were also identified. Through the prediction of the online bioinformatics tool starBase and the verification of dual-luciferase reporter as-

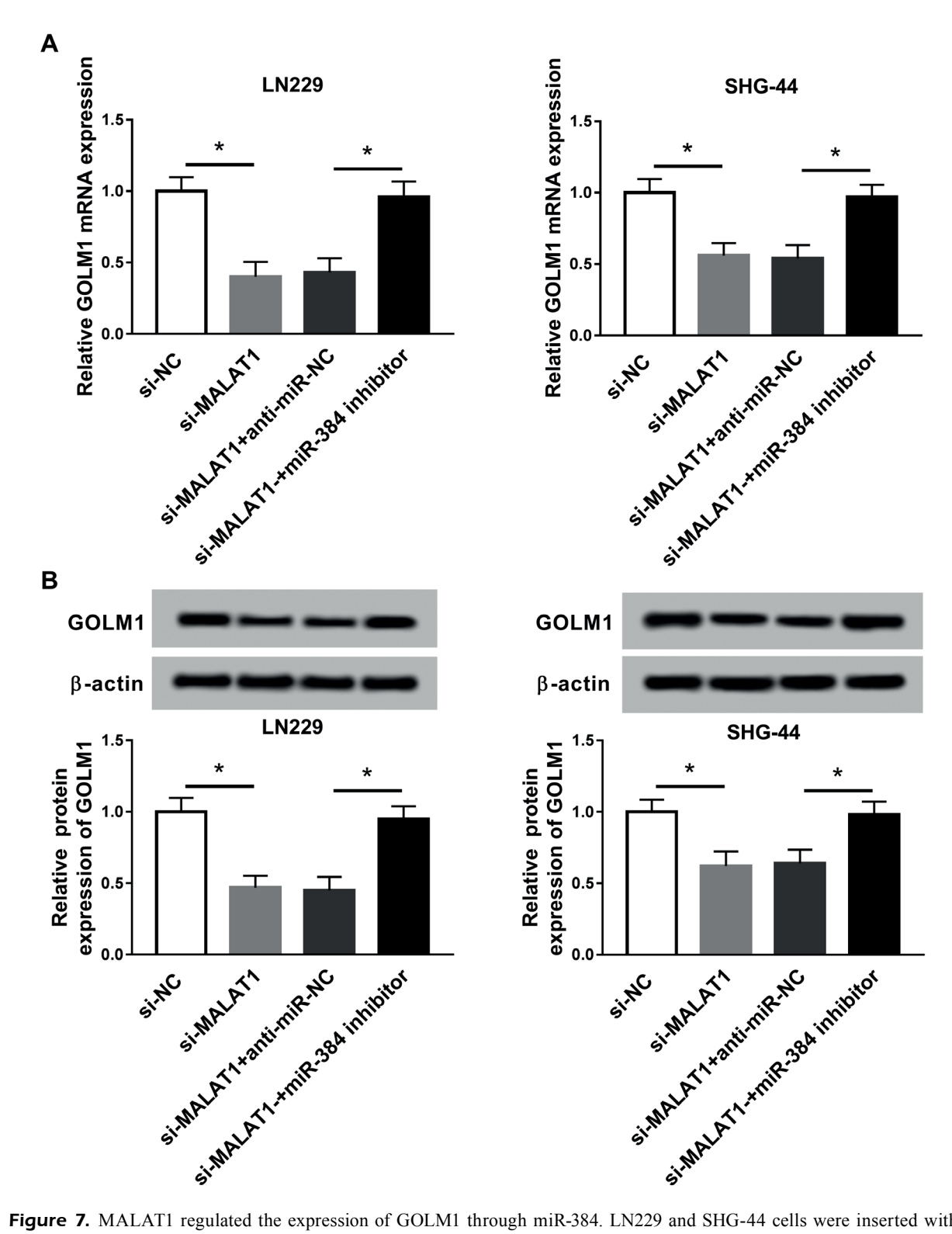


Figure 7. MALAT1 regulated the expression of GOLM1 through miR-384. LN229 and SHG-44 cells were inserted with si-MALAT1, si-NC, si-MALAT1+miR-384 inhibitor or si-MALAT1+anti-miR-NC. (**A** and **B**) The expression of GOLM1 at mRNA and protein levels was monitored using qRT-PCR and Western blot. *p < 0.05.

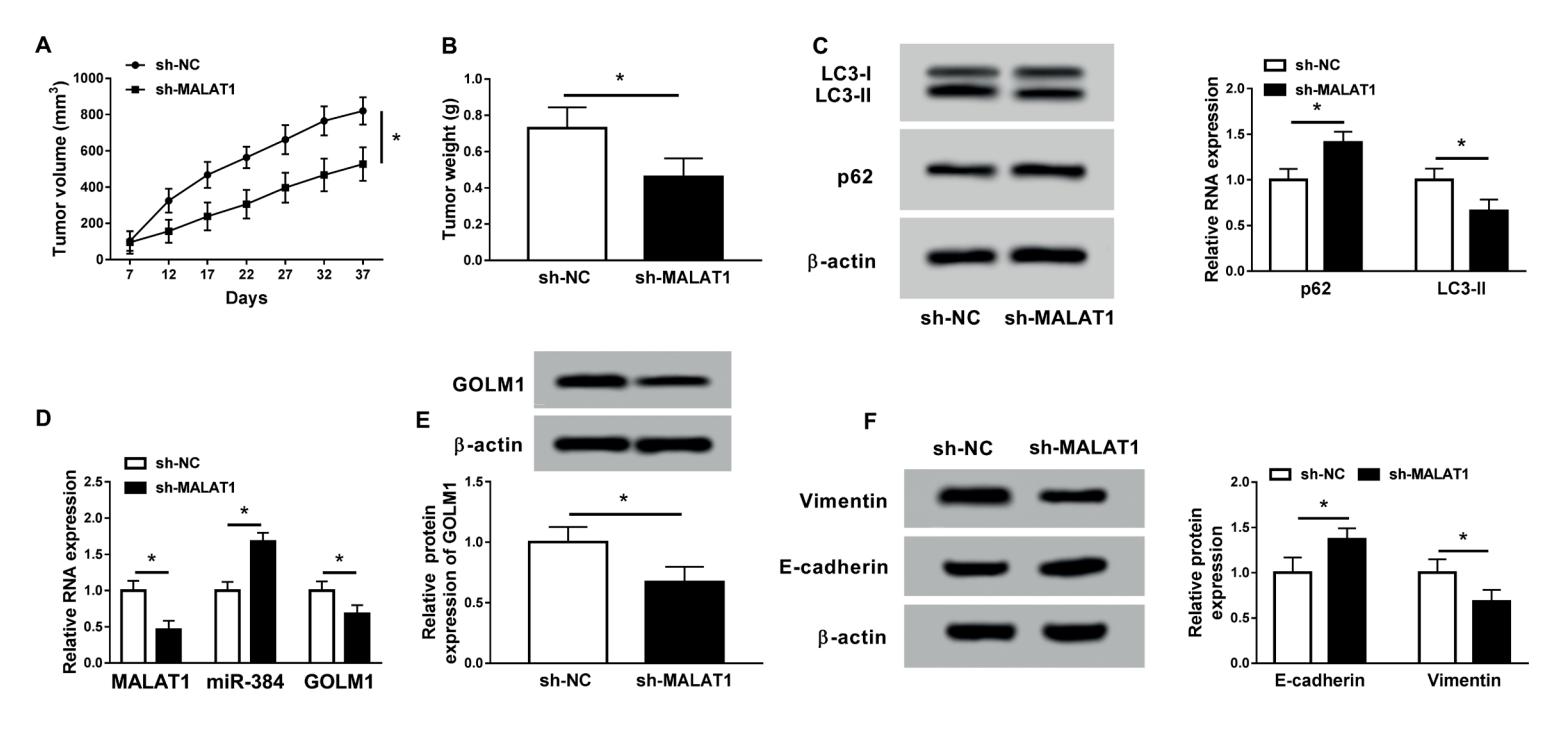


Figure 8. MALAT1 knockdown blocked tumor growth and development *in vivo*. (**A**) The tumor volume was recorded every 5 days. (**B**) The tumor weight was measured at 37-day post injection. (**C**) The protein levels of LC3-II and p62 were detected in removed tumor tissues. (**D**) The expression of MALAT1, miR-384 and GOLM1 in tumor tissues was checked using qRT-PCR. (**E** and **F**) The protein levels of GOLM1, Vimentin and E-cadherin were monitored using Western blot. *p < 0.05.

say, GOLM1 was indicated as a target of miR-384, which was negatively correlated with miR-384 expression in glioma tissues. The role of GOLM1 in glioma was partly explored before, and the results suggested that the expression level of GOLM1 was strengthened in glioma tissues and cells. Overexpression of GOLM1 promoted the proliferation, migration and invasion, while GOLM1 silence alleviated these malignant behaviors ³². In line with this study, our research exhibited a similar consequence. Besides, we proved that GOLM1 knockdown inhibited autophagy in glioma cells.

Conclusions

Collectively, the abundance of MALAT1 was abnormally enhanced in glioma tissues and cell lines. This study first put forward that MALAT1 knockdown weakened cell migration and invasion by depleting autophagy via miR-384/GOLM1 regulatory axis *in vitro* and *in vivo*. This newly identified MALAT1/miR-384/GOLM1 axis might provide new insights into the mechanism of glioma metastasis, and MALAT1 may be a promising therapeutic target for glioma in the future.

Conflict of Interests

The Authors declare that they have no conflict of interests.

References

- 1) JIANG T, MAO Y, MA W, MAO Q, YOU Y, YANG X, JIANG C, KANG C, LI X, CHEN L, QIU X, WANG W, LI W, YAO Y, LI S, LI S, WU A, SAI K, BAI H, LI G, CHEN B, YAO K, WEI X, LIU X, ZHANG Z, DAI Y, LV S, WANG L, LIN Z, DONG J, XU G, MA X, CAI J, ZHANG W, WANG H, CHEN L, ZHANG C, YANG P, YAN W, LIU Z, HU H, CHEN J, LIU Y, YANG Y, WANG Z, WANG Y, YOU G, HAN L, BAO Z, LIU Y, WANG Y, FAN X, LIU S, LIU X, WANG Y, WANG Q, Chinese Glioma Cooperative Group (CGCG). CGCG clinical practice guidelines for the management of adult diffuse gliomas. Cancer Lett 2016; 375: 263-273.
- DEWITT JC, JORDAN JT, FROSCH MP, SAMORE WR, IAFRATE AJ, LOUIS DN, LENNERZ JK. Cost-effectiveness of IDH testing in diffuse gliomas according to the 2016 WHO classification of tumors of the central nervous system recommendations. Neuro Oncol 2017; 19: 1640-1650.
- ZHENG J, LIU X, XUE Y, GONG W, MA J, XI Z, QUE Z, LIU Y. TTBK2 circular RNA promotes glioma malignancy by regulating miR-217/HNF1beta/Derlin-1 pathway. J Hematol Oncol 2017; 10: 52.

- 4) Louis DN, Perry A, Reifenberger G, von Deimling A, Figarella-Branger D, Cavenee WK, Ohgaki H, Wiestler OD, Kleihues P, Ellison DW. The 2016 World Health Organization Classification of Tumors of the Central Nervous System: a summary. Acta Neuropathol 2016; 131: 803-820.
- 5) STUPP R, BRADA M, VAN DEN BENT MJ, TONN JC, PENTHEROUDAKIS G; ESMO Guidelines Working Group. High-grade glioma: ESMO Clinical Practice Guidelines for diagnosis, treatment and follow-up. Ann Oncol 2014; 25 Suppl 3: iii93-101.
- Berges R, Balzeau J, Peterson AC, Eyer J. A tubulin binding peptide targets glioma cells disrupting their microtubules, blocking migration, and inducing apoptosis. Mol Ther 2012; 20: 1367-1377.
- Gulati S, Jakola AS, Johannesen TB, Solheim O. Survival and treatment patterns of glioblastoma in the elderly: a population-based study. World Neurosurg 2012; 78: 518-526.
- Li P, He J, Yang Z, Ge S, Zhang H, Zhong Q, Fan X. ZNNT1 long noncoding RNA induces autophagy to inhibit tumorigenesis of uveal melanoma by regulating key autophagy gene expression. Autophagy 2019 Sep 3:1-14. doi: 10.1080/15548627.2019.1659614. [Epub ahead of print]
- ZHAO Y, ZHAO L, LI J, ZHONG L. Silencing of long noncoding RNA RP11-476D10.1 enhances apoptosis and autophagy while inhibiting proliferation of papillary thyroid carcinoma cells via microR-NA-138-5p-dependent inhibition of LRRK2. J Cell Physiol 2019; 234: 20980-20991.
- ZHANG N, LI Z, BAI F, ZHANG S. PAX5-induced upregulation of IDH1-AS1 promotes tumor growth in prostate cancer by regulating ATG5-mediated autophagy. Cell Death Dis 2019; 10: 734.
- WANG CZ, YAN GX, DONG DS, XIN H, LIU ZY. LncRNA-ATB promotes autophagy by activating Yes-associated protein and inducing autophagy-related protein 5 expression in hepatocellular carcinoma. World J Gastroenterol 2019; 25: 5310-5322.
- 12) Wang X, Liu W, Wang P, Li S. RNA interference of long noncoding RNA HOTAIR suppresses autophagy and promotes apoptosis and sensitivity to cisplatin in oral squamous cell carcinoma. J Oral Pathol Med 2018; 47: 930-937.
- CHOI J, JUNG W, KOO JS. Expression of autophagy-related markers beclin-1, light chain 3A, light chain 3B and p62 according to the molecular subtype of breast cancer. Histopathology 2013; 62: 275-286.
- Lee W, Lim S, Kim Y. The role of myosin II in glioma invasion: a mathematical model. PLoS One 2017; 12: e0171312.
- 15) FARIN A, SUZUKI SO, WEIKER M, GOLDMAN JE, BRUCE JN, CANOLL P. Transplanted glioma cells migrate and proliferate on host brain vasculature: a dynamic analysis. Glia 2006; 53: 799-808.
- Mowers EE, Sharifi MN, MacLEDD KF. Autophagy in cancer metastasis. Oncogene 2017; 36: 1619-1630.

- 17) SUN WL, KANG T, WANG YY, SUN JP, LI C, LIU HJ, YANG Y, JIAO BH. Long noncoding RNA OIP5-AS1 targets Wnt-7b to affect glioma progression via modulation of miR-410. Biosci Rep 2019; 39(1). pii: BSR20180395.
- 18) Ma Y, Zhou G, Li M, Hu D, Zhang L, Liu P, Lin K. Long noncoding RNA DANCR mediates cisplatin resistance in glioma cells via activating AXL/ PI3K/Akt/NF-kappaB signaling pathway. Neurochem Int 2018; 118: 233-241.
- 19) Li X, Zhang H, Wu X. Long noncoding RNA DLX6-AS1 accelerates the glioma carcinogenesis by competing endogenous sponging miR-197-5p to relieve E2F1. Gene 2019; 686: 1-7.
- YANG L, BAI HS, DENG Y, FAN L. High MALAT1 expression predicts a poor prognosis of cervical cancer and promotes cancer cell growth and invasion. Eur Rev Med Pharmacol Sci 2015; 19: 3187-3193.
- 21) YUAN J, XU XJ, LIN Y, CHEN QY, SUN WJ, TANG L, LIANG QX. LncRNA MALAT1 expression inhibition suppresses tongue squamous cell carcinoma proliferation, migration and invasion by inactivating PI3K/Akt pathway and downregulating MMP-9 expression. Eur Rev Med Pharmacol Sci 2019; 23: 198-206.
- 22) Guo C, Wang X, Chen LP, Li M, Li M, Hu YH, Ding WH, Wang X. Long non-coding rna malat1 regulates ovarian cancer cell proliferation, migration and apoptosis through Wnt/Beta-catenin signaling pathway. Eur Rev Med Pharmacol Sci 2018; 22: 3703-3712.
- 23) Li Z, Dou P, Liu T, HE S. Application of long noncoding RNAs in osteosarcoma: biomarkers and therapeutic targets. Cell Physiol Biochem 2017; 42: 1407-1419.
- GEBERT LFR, MACRAE IJ. Regulation of microRNA function in animals. Nat Rev Mol Cell Biol 2019; 20: 21-37.
- 25) MA Q, QI X, LIN X, LI L, CHEN L, HU W. LncRNA SNHG3 promotes cell proliferation and invasion through the miR-384/hepatoma-derived growth factor axis in breast cancer. Hum Cell 2019 Oct 4. doi: 10.1007/s13577-019-00287-9. [Epub ahead of print]
- 26) Wang Y, Huang H, Li Y. Knocking down miR-384 promotes growth and metastasis of osteosar-coma MG63 cells by targeting SLBP. Artif Cells Nanomed Biotechnol 2019; 47: 1458-1465.
- 27) Gu G, Wang L, Zhang J, Wang H, Tan T, Zhang G. MicroRNA-384 inhibits proliferation migration and invasion of glioma by targeting at CDC42. Onco Targets Ther 2018; 11: 4075-4085.

- ZHENG J, LIU X, WANG P, XUE Y, MA J, QU C, LIU Y. CRNDE promotes malignant progression of glioma by attenuating miR-384/PIWIL4/STAT3 axis. Mol Ther 2016; 24: 1199-1215.
- 29) Ambros V. The functions of animal microRNAs. Nature 2004; 431: 350-355.
- Yan G, Ru Y, Wu K, Yan F, Wang Q, Wang J, Pan T, ZHANG M, Han H, Li X, Zou L. GOLM1 promotes prostate cancer progression through activating PI3K-AKT-mTOR signaling. Prostate 2018; 78: 166-177.
- LIU X, CHEN L, ZHANG T. Increased GOLM1 expression independently predicts unfavorable overall survival and recurrence-free survival in lung adenocarcinoma. Cancer Control 2018; 25: 1073274818778001.
- 32) Xu R, Ji J, Zhang X, Han M, Zhang C, Xu Y, Wei Y, Wang S, Huang B, Chen A, Zhang D, Zhang Q, Li W, Jiang Z, Wang J, Li X. PDGFA/PDGFRalpha-regulated GOLM1 promotes human glioma progression through activation of AKT. J Exp Clin Cancer Res 2017; 36: 193.
- 33) LAZOVA R, CAMP RL, KLUMP V, SIDDIOUI SF, AMARAVA-DI RK, PAWELEK JM. Punctate LC3B expression is a common feature of solid tumors and associated with proliferation, metastasis, and poor outcome. Clin Cancer Res 2012; 18: 370-379.
- 34) Huang Z, Huang L, Shen S, Li J, Lu H, Mo W, Dang Y, Luo D, Chen G, Feng Z. Sp1 cooperates with Sp3 to upregulate MALAT1 expression in human hepatocellular carcinoma. Oncol Rep 2015; 34: 2403-2412.
- 35) LI Z, XU C, DING B, GAO M, WEI X, JI N. Long non-coding RNA MALAT1 promotes proliferation and suppresses apoptosis of glioma cells through derepressing Rap1B by sponging miR-101. J Neurooncol 2017; 134: 19-28.
- 36) HAN Y, ZHOU L, WU T, HUANG Y, CHENG Z, LI X, SUN T, ZHOU Y, DU Z. Downregulation of IncRNA-MALAT1 affects proliferation and the expression of stemness markers in glioma stem cell line SHG139S. Cell Mol Neurobiol 2016; 36: 1097-1107.
- 37) XIANG J, GUO S, JIANG S, XU Y, LI J, LI L, XIANG J. Silencing of long non-coding RNA MALAT1 promotes apoptosis of glioma cells. J Korean Med Sci 2016; 31: 688-694.
- 38) Fu Z, Luo W, Wang J, Peng T, Sun G, Shi J, Li Z, Zhang B. Malat1 activates autophagy and promotes cell proliferation by sponging miR-101 and upregulating STMN1, RAB5A and ATG4D expression in glioma. Biochem Biophys Res Commun 2017; 492: 480-486.